

# Dynamic oscillatory cluster ordering of self-propelled droplets

Shinpei Tanaka\*

*Graduate School of Integrated Arts and Sciences, Hiroshima University,  
1-7-1 Kagamiyama, Higashi-Hiroshima 739-8521, Japan*

Takeshi Kano

*Research Institute of Electrical Communication, Tohoku University,  
2-1-1 Katahira, Aoba-ku, Sendai 980-8577, Japan*

We report here a peculiar dynamically ordered state of clustering droplets of a mixture of organic solvent. These droplets are driven by the solutal Marangoni effect on the surface of aqueous surfactant solution. They form temporal ring clusters which start collapsing immediately after its formation. This process is repeated for more than several hours with the period of 5–20 minutes. We propose an inhomogeneous force model to phenomenologically understand the basic mechanism of this dynamics, where the forces acting on each particle are controlled differently. This droplet system offers a simple, non-biological experimental model for the study of complex dynamical states realized by a group of self-propelled particles.

PACS numbers: 68.03.Cd 82.40.Bj 82.40.Ck 05.65.+b

arXiv:1706.00154v1 [cond-mat.soft] 1 Jun 2017

---

\* shinpei@hiroshima-u.ac.jp

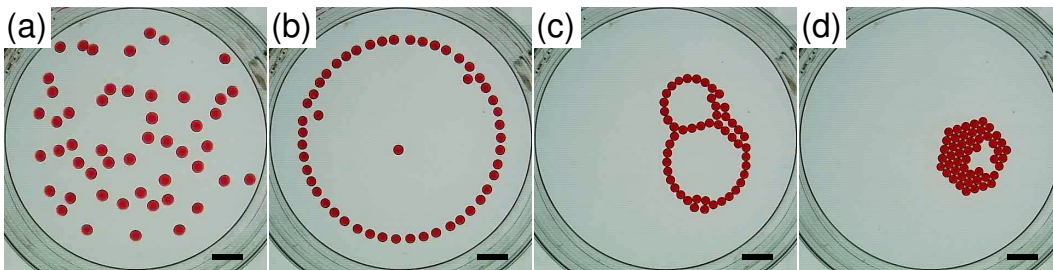


FIG. 1. The modes of motion seen in a system of  $N = 50$  in sequence. (a) Random, intermittent motion. (b) A ring of droplets where droplets vibrated between others. (c) The characteristic cluster oscillation. (d) A final static crystal. The scale bar is 10 mm.

Biological functions sometimes arise from a cluster of active elements. For example, it has been proposed that the swarming behaviors of bacteria is beneficial to each bacterium in an occasion such as a food intake or resisting starvation [1]. There the motility and communication of bacteria play important roles to initiate coordinated behaviors. It has been proposed that the complex interaction among them has been evolving to optimize the required functions, which may have even led to the multicellularity [2].

To fully understand these collective behaviors seen in biological systems, it is important to construct non-biological systems capable to model them. It is now well-known that the swarming phenomena are not limited in biological systems, but can be also seen in many non-biological motile systems [3–5]. Their connection to the biological systems has been studied by many researchers so far [6].

Beyond the relatively simple pattern formations observed so far in the non-biological systems, however, it is a challenging task to find physical systems capable to exhibit complex and dynamical collective patterns comparable to biological systems. Ikura et al. found the collective motion of camphor boats, exhibiting a billiard-like transfer of motion if confined in a narrow channel [7, 8]. Soh et al. reported that gel particles containing camphor created characteristic dynamical ordering [9].

We have recently shown that droplets of alkyl salicylate floating on aqueous surfactant solution exhibit a stable self-propulsion [10]. Here we report collective behaviors of similar droplet systems, where droplets show much more complex modes of motion than those observed in non-biological systems reported so far. Our droplets contain two liquids, ethyl salicylate (ES) and paraffin liquid, and the dissolution of ES produces a surface tension gradient around the droplet that propels it [10]. Thus ES is used as a fuel, whereas inert paraffin liquid composes a droplet body. Although this droplet system consists of simple components, it can exhibit various complex collective behaviors, which actually resemble wiggling motion of earthworms.

In this report, we propose inhomogeneous forces as a tool to understand the complex behaviors of droplets. Our droplets interact with each other via the field around them created by themselves. There the field created by an isolated particle is not necessarily the same with the one created by the same particle in a cloud of particles. In other words, the superposition principle of the interaction does not necessarily hold. Therefore this way of the interparticle interaction can be beyond homogeneous; homogeneous here means that all the elements share the same type of interaction depending only on the distance between them. The interaction becomes inhomogeneous if the local environment around an element differs from others. In the first part of this report, we describe the experimental observations of our droplet system. Then in the second part, we show that a simple inhomogeneous model can reproduce the observations at least in part.

Droplets of ethyl salicylate (ES, Tokyo Chemical Industry, Tokyo) used in this study contained 30 wt% of paraffin liquid (Sigma-Aldrich, Tokyo). The volume of a droplet was 10  $\mu\text{l}$ . The droplets were placed on the surface of 30 ml aqueous sodium dodecyl sulfate (SDS, Tokyo Chemical Industry) solution in a glass dish of 86 mm in inner diameter. The concentration of SDS was fixed at 35 mM. A glass cover was used without a tight sealing. The number of droplets,  $N$ , was 1 – 200. The elapsed time,  $t$ , was measured from the time when all the droplets were placed on the aqueous surface. The droplets were dyed with Oil red O (Nakarai tesque, Tokyo). The chemicals were used as supplied.

The motion of droplets was recorded using a CMOS camera (L-835, Hozan, Osaka) as a movie. The sample as well as the camera were placed in a temperature-controlled box, where the temperature was controlled at  $21.0 \pm 0.2^\circ\text{C}$  using a heater. From a recorded movie, images of  $640 \times 480$  pixels were extracted and the position of droplets was detected using a software, ImageJ (<http://rsb.info.nih.gov/ij/>). By differentiating the position numerically, the velocity was calculated.

Figure 1 shows four typical structures seen in sequence in a system of  $N = 50$  (see also the Supplementary Material, SM). At first the droplets are in random, intermittent motion [Fig. 1(a) and mov-1, SM] but gradually form a ring

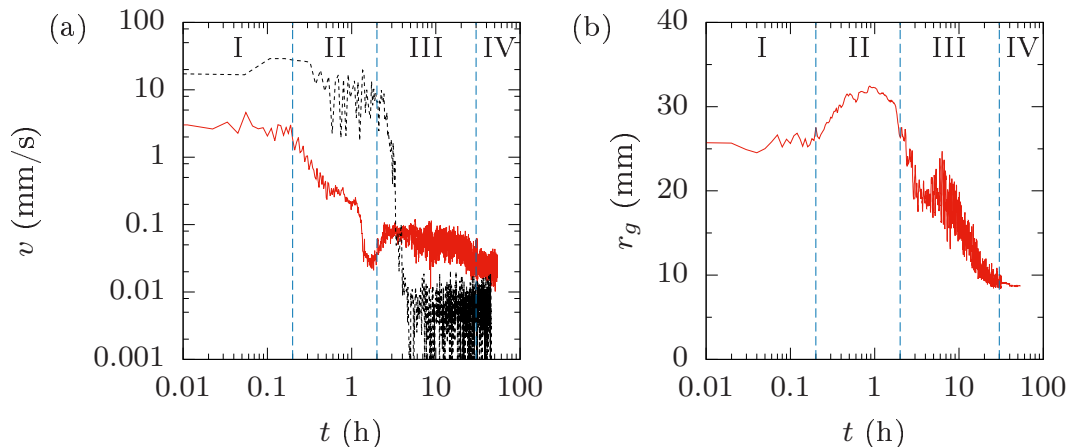


FIG. 2. (a) The average speed of droplets,  $v$ . The solid red line shows the values when  $N = 50$ ; the dashed black line shows the values when  $N = 1$  under the same condition. (b) The radius of gyration,  $r_g$ , of the droplet distribution. The stages I to IV corresponds with the motion patterns shown in Fig. 1.

where each droplet vibrates between the others [Fig. 1(b) and mov-2, SM]. We refer in this report that this oscillation of a single droplet as droplet oscillation. The period of droplet oscillation is typically several seconds. The ring shown in Fig 1(b) is the result of a circular dish used. When in a larger square dish, the droplets form clusters of typically  $N \sim 10$  (mov-3, SM).

Then the ring collapses into a cluster and a periodic wiggling motion of the cluster begins [Fig. 1(c) and mov-4, SM]. We refer this oscillatory motion of a cluster as cluster oscillation. This cluster oscillation can be observed in a cluster as small as  $N = 5$ . When  $N$  is larger than about 10, this cluster oscillation looks a periodic wiggling motion. The period of cluster oscillation is about 10 minutes, much longer than that of droplet oscillation. This cluster oscillation was also observed in a smaller (60 mm) and larger (200 mm) dish (mov-5, SM). Finally, the droplets were aligned on a hexagonal lattice to form a crystal with well-defined facets [Fig. 1(d) and mov-6, SM].

Figure 2(a) shows the average speed of a droplet in a system of  $N = 50$  (red solid line) and of an isolated droplet ( $N = 1$ , black dashed line) under the same condition. It shows that the droplets' motion was suppressed at first when many droplets coexist. However, even after the isolated droplet stopped, droplets in a system of  $N = 50$  kept moving, though slowly. This slow movement corresponds to the cluster oscillation shown in Fig. 1(c) and Fig. 3.

Figure 2(b) shows the radius of gyration,  $r_g$ , calculated as the root mean square distance of all droplets from the center of mass of the droplet distribution. It showed a maximum and then decreased to the value of a compact cluster shown in Fig. 1(d). Using Fig. 2(a) and (b), we divide the process of dynamic ordering into four stages, where stages I to IV correspond with the patterns (a)-(d) shown in Fig. 1. The reproducibility of the process was high though the time of transition from a stage to the next depends on the conditions. In the stage I,  $v$  is the highest and the droplets are randomly distributed. In the stage II,  $v$  decreases rapidly and  $r_g$  reaches the maximum reflecting the ring structure along the wall [Fig. 1(b)]. After  $v$  reaches the minimum, the ring collapses and the cluster oscillation begins [Fig. 1(c)] in the stage III. There  $v$  is recovered to a certain value. The stage III continued for about 30 hours in the sample shown in Fig. 1. During the stage III,  $r_g$  keeps oscillating. In the late stage of the stage III, the wiggling cluster shrinks gradually. In the stage IV, the cluster becomes a crystal.

Figure 3 shows snapshots of the cluster oscillation seen in a system of  $N = 50$  (mov-4, SM). When  $N \gtrsim 10$ , the motion pattern is in general the repeated formation and collapse of rings as follows. First, a ring cluster (which was smaller than the one in the stage II) is formed with a thread of droplets [Fig. 3(a)]. It breaks at a point [Fig. 3(a)], then the thread starts shrinking with forming local small rings within it [Fig. 3(b)]. The local rings sometimes merge while another rings are forming continuously [Fig. 3(c)]. Finally one ring becomes dominant and a large ring cluster is recovered [Fig. 3(d)]. Then the process is repeated.

Figure 4 shows the oscillation of the cluster shown in Fig. 3. The velocity autocorrelation function [Fig. 4(a)] has a negative part after a rapid decrease at around  $t' \simeq 5$  (min), reflecting the circular motion of a droplet in the cluster. The radius of gyration of the cluster [Fig. 4(b)] exhibits clear oscillation, with the period of about 15 minutes in this case.

The complex cluster oscillation (periodic wiggling) may be decomposed into simpler ones, if  $N$  is small. Figure 5(a) shows the small clusters formed in a system of  $N = 25$ . Other conditions were the same as the one shown in Fig. 1. The motion of the cluster "2" is depicted in sequence in Fig. 5(b), where a droplet in between four droplets moved

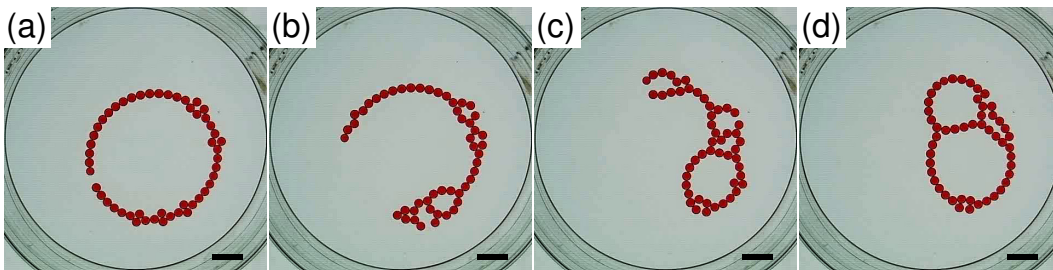


FIG. 3. Snapshots of droplets in the cluster oscillation ( $N = 50$ ). The elapsed time was  $t = 8$  h. The time elapsed from (a) was, (a) 0 s, (b) 116 s, (c) 336 s, and (d) 504 s. The scale bar is 10 mm.

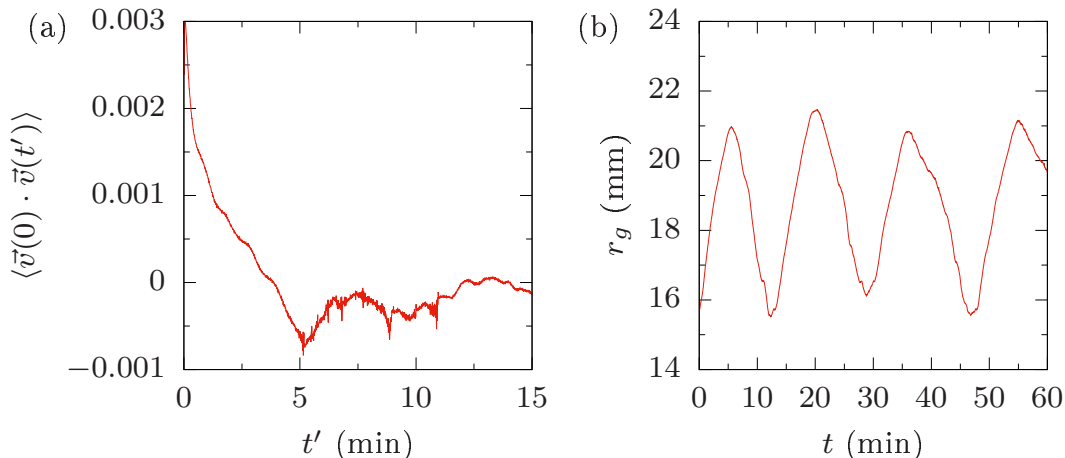


FIG. 4. (a) The velocity autocorrelation function of a droplet in the cluster shown in Fig. 3. (b) The oscillation of  $r_g$  of the same cluster.  $t = 0$  (min) here corresponds with  $t = 8$  h in Fig. 2.

back-and-forth with the period of about 10 minutes [Fig. 5(c), “2” and mov-7, SM]. Although it is not like “wiggling” for this small cluster, it is a minimum cluster oscillation with the similar period of oscillation.

The oscillation of this small cluster was also seen clearly in the velocity autocorrelation function [Fig. 5(d)]. Moreover, it shows another rapid oscillation [Fig. 5(d), inset] with the period of about 10 s. This faster oscillation corresponds with a remaining droplet oscillation seen mainly in the stage I and II, which decays gradually while the cluster oscillation persists.

On the other hand, the cluster with four droplets, assigned with “1”, was in a translational motion [Fig. 5(c), “1”]. An isolated droplet, “3”, was in a slower translational motion. Thus the clusters can be in a different dynamical state even if they are in the same dish.

Let us summarize the observation on the cluster oscillation and add some additional information. (1) The cluster oscillation is a slow mode of motion that appears when the unbalanced surface tension gradient, that is, the Marangoni effect, mostly decays. Only the existence of neighboring droplets can induce the net motion. (2) The cluster oscillation is long-lasting motion. In the example shown in Fig. 3, it continued about 30 hours; in the example shown in Fig. 5 it lasted for more than two weeks. (3) The cluster oscillation is robust against  $N$ , when the droplets can interact with each other. We observed this mode of motion when  $N = 5 - 200$  so far.

The observations (1) to (3) suggest that the cluster oscillation is caused by the characteristic interaction among droplets after the main self-propulsion force decays. Judging from the complex cluster motion observed, however, this interaction is not the simple one depending only on the relative arrangement between two particles, but is active one depending also on the local environment and possibly on the internal state of the particle. This is crucially different from solid particle systems such as camphor boats, where it is difficult for the elements to have the time-dependent internal state. Moreover, it has been proposed that the existence of internal states can produce variety of dynamic patterns [11].

Regarding the interaction, the experiments suggest that there are at least three types of interaction among droplets: (a) an attraction between droplets due to the capillary interaction, which eventually stabilizes close-packed, crystalline

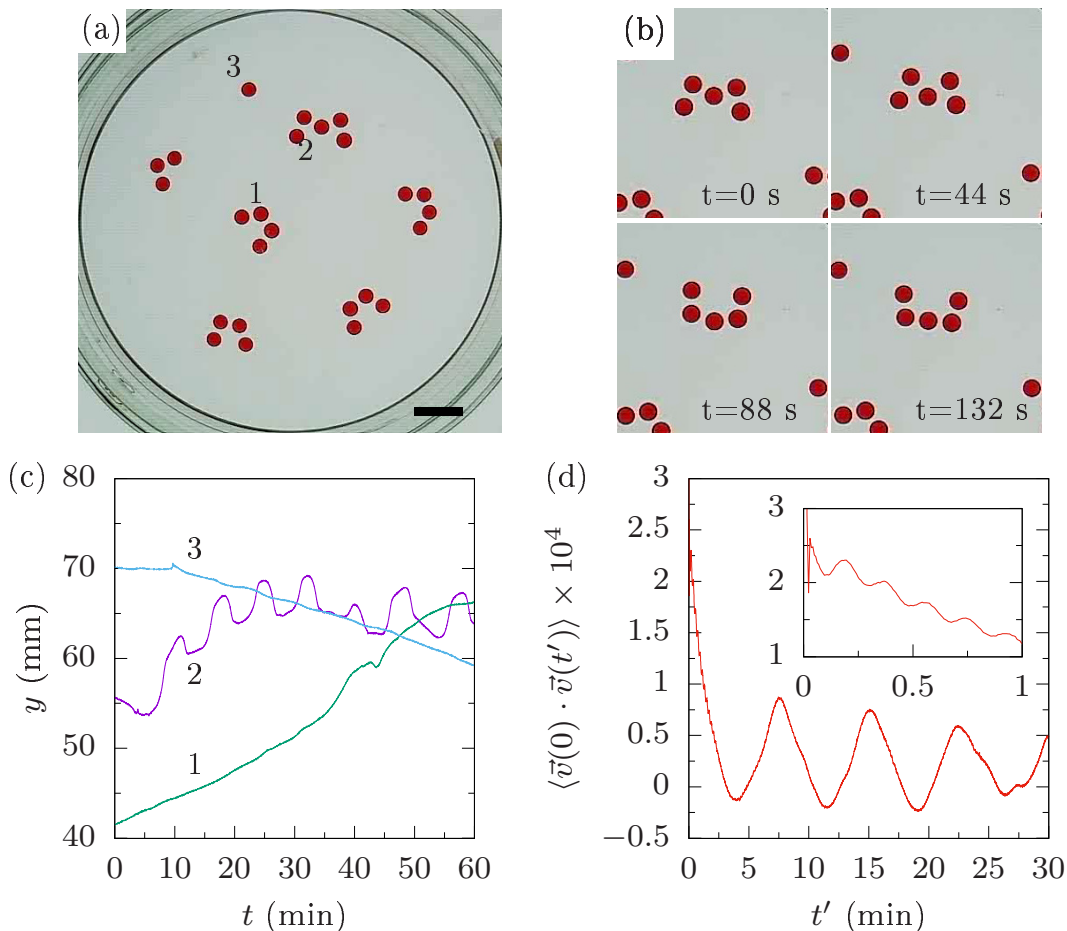


FIG. 5. The dynamic states of small clusters ( $N = 25$ ). (a) Clusters observed at  $t = 5$  h. The scale bar is 10 mm. (b) The cluster oscillation in a cluster of  $N = 5$ . (c) The change in the  $y$ -coordinate of the droplets. The figures represent a droplet shown in (a). (d) The velocity autocorrelation function averaged over all the droplets. Inset is an enlarged view in the region of  $t' < 1$  min.

aggregates; (b) a short-range (possibly microscopic) unknown mechanism preventing the droplets' coalescence; (c) a time-dependent interaction causing the cluster oscillation.

There is additional information regarding (c). When the droplets are confined in a linear channel, they do not form a chain but keep a certain distance with occasional droplet oscillation (mov-8 and mov-9, SM). Since the Marangoni flow is restricted to the direction parallel to the channel and is known to induce repulsion between particles [9], it is the confinement that makes the Marangoni-flow-induced repulsion dominant, and prevent the cluster formation. Therefore this suggests that the interaction (c) consists partly of the directional Marangoni-flow-induced repulsion.

It is considered that the interaction (c) reflects the surrounding field produced as a consequence of the history of droplets' motion. Thus it seems not possible to reproduce the observed phenomena by assuming that all the particles interact with each other via homogeneous interaction rules. Therefore, we test a simple phenomenological model where each elements interact with each other differently. This approach will tell us important clues to understand the essential mechanisms of the cluster oscillation.

Under the assumption of the overdamped limit, we model the equation of motion of a particle as in dimensionless form,

$$\mathbf{v}_i = \sum_{j \neq i} (-k_{ij} R_{ij}^{-1} + R_{ij}^{-2}) \mathbf{e}_{ij} + f_i \mathbf{n}_i \quad (1)$$

$$\tau \dot{\mathbf{n}}_i = \{\mathbf{n}_i \times (\mathbf{v}_i / v_i)\} \times \mathbf{n}_i, \quad (2)$$

where  $\mathbf{v}_i$  is the velocity of  $i$ -th particle and  $\mathbf{e}_{ij}$  is the unit vector pointing from  $j$ -th particle to  $i$ -th particle.  $R_{ij}$  and  $k_{ij}$  are the distance and the attraction strength between  $i$ -th particle and  $j$ -th particle, respectively. We assume

simple power law attraction and repulsion between particles. The propulsion force,  $f_i$ , acts in the direction of the unit vector  $\mathbf{n}_i$  that represents the internal state of  $i$ -th particle. We adopt a model proposed by Shimoyama et al. [12] for the change of  $\mathbf{n}_i$  [Eq. (2)] with the relaxation time  $\tau$ .

The inhomogeneity enters in  $k_{ij}$  and  $f_i$ , thus the number of parameters increases quickly with  $N$ . The model, therefore, is applicable only to small clusters, and is useful to see how the inhomogeneous forces induce their cluster oscillation.

We nondimensionalized the variables using the diameter of a droplet ( $d^* = 3 \times 10^{-3}$  m), the average speed ( $v^* = 2 \times 10^{-5}$  m/s), and the friction constant ( $\zeta^* = 1 \times 10^{-5}$  kg/s) estimated according to the Stokes law. Then the unit of time was  $t^* = 150$  s and the typical force,  $f^* = \zeta^* v^*$ , was nondimensionalized as 1. The equations (1) and (2) were solved using the fourth order Runge-Kutta method with the time step of 0.001.

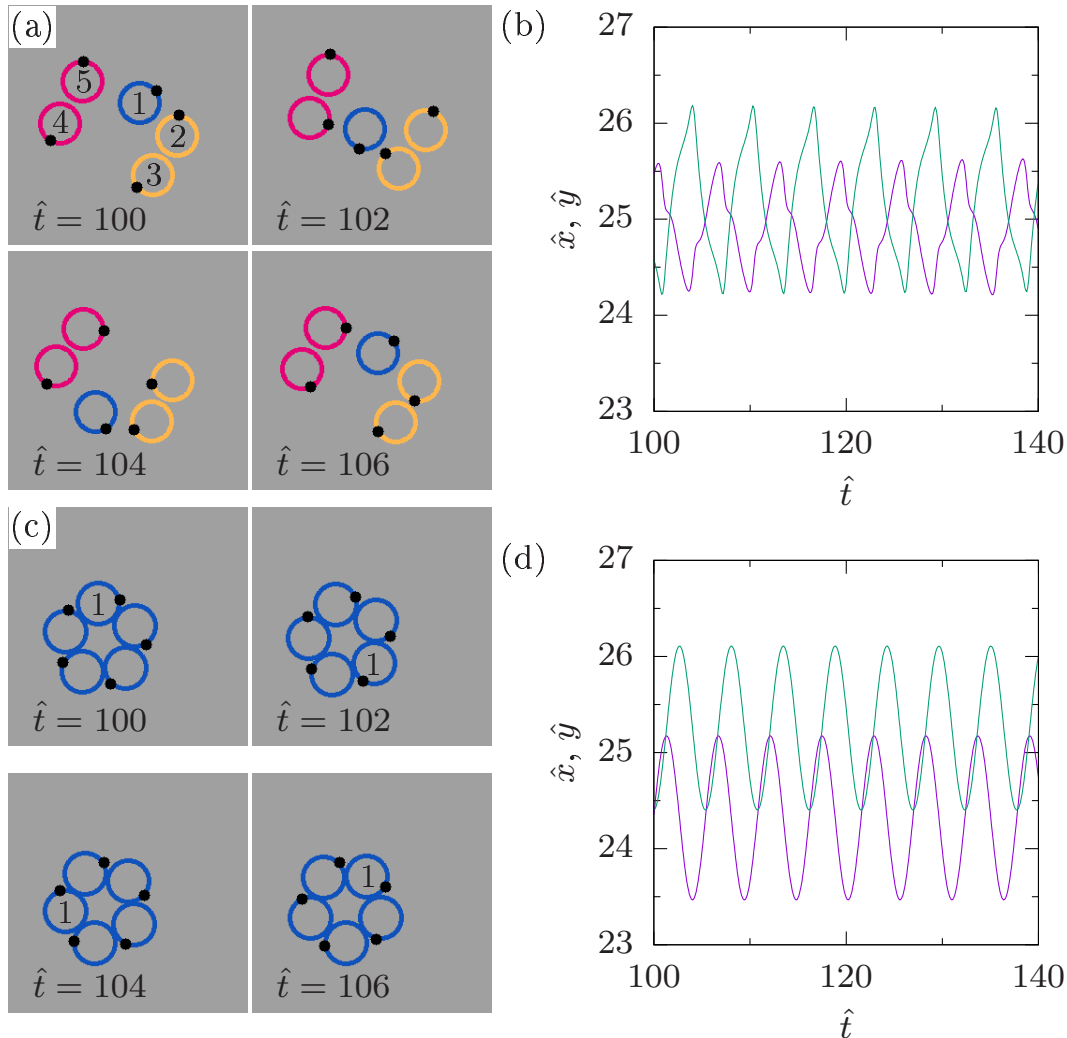


FIG. 6. A 5-element cluster obtained by the simulation with the inhomogeneous forces, (a), and with the homogeneous forces, (c).  $\tau = 0.1$ . The inhomogeneous interaction in (a) is:  $k_{ij} = 0.8$  for  $i = 1$  or  $j = 1$ , or  $(i, j) = (2, 3), (3, 2)$ , or  $(i, j) = (4, 5), (5, 4)$ ;  $k_{ij} = 0.3$  for other combinations of  $(i, j)$ . The propulsion force was  $f_1 = 1.0$  and  $f_i = 0$  for  $i \neq 1$ . In (c),  $k_{ij} = 0.8$  for  $i \neq j$ , and  $f_i = 1.0$  for all  $i$ . The  $\hat{x}$  and  $\hat{y}$  coordinates of the blue element ( $i = 1$ ) in (a) are plotted in (b), and those in (c) are plotted in (d). A black dot on the elements represents  $\mathbf{n}_i$ .

Figure 6 shows an example of a 5-element system. In Fig. 6(a), the attraction between pink particles and orange particles was weaker than others, and only the blue particle was propelled. Then the particles self-organized into an oscillatory state similar to the one shown in Fig. 5(b) [Fig. 6(b) and mov-10, SM]. This oscillatory state was not sensitive to the difference of attraction among elements (mov-11 and mov-12, SM). The nondimensional period of the oscillation, about 6, and the relaxation time, 0.1, correspond to 15 minutes and 15 s, respectively. They are close to the observed period of, respectively, the cluster oscillation and the droplet oscillation [Fig. 5(c) and (d)].

On the other hand, if the forces are homogeneous, that is, all the elements interact and are propelled similarly, they start to move in a circular motion as shown in Fig. 6(c) and (d) (mov-13, SM), and do not show back-and-forth oscillation. Thus the inhomogeneity of the forces plays a crucial role in the dynamic oscillatory state.

We could also reproduce other cluster motions including a four droplets translation [cluster 1 in Fig. 5(a) and mov-14, SM] and a rotation of S-shaped chain observed in other experiments (mov-15 and mov-16, SM). However, so far the wiggling motion seen in a larger cluster like the one shown in Fig. 3 has not been reproduced yet. In our model, the interaction  $k_{ij}$  and the propulsion  $f_i$  are fixed throughout a simulation. In the wiggling motion, however, the value of these parameters might also change with time according to the situation.

In conclusions, we found a self-propelled droplet system driven by the solutal Marangoni effect, where the droplets self-organized into a characteristic dynamic oscillatory state. The interaction among droplets was essential for this dynamic oscillatory state, since this state appeared only with neighboring particles and in a stage where a single particle motion decayed mostly.

We tested a model which did not assume the homogeneous forces acting on elements. The model reproduced a 5-element oscillation well, as well as some behaviors of small clusters. This suggests the inhomogeneity of the interaction as well as the propulsion forces, due to the Marangoni effect mediated by the field around the elements, which does not necessarily obey the superposition principle. This is essentially different from a passive material where the interaction potential is pre-determined.

Our system needs to be investigated further, especially in terms of the active, inhomogeneous interaction, not only for understanding the mechanisms of the dynamic ordering phenomena, but also for designing life-mimicking systems. We believe that our experimental system can be an ideal model system for this direction of investigation, for its simplicity, robustness, and long-lasting motions.

- 
- [1] D. Kaiser, *Nature Rev. Microbiol.*, **1**, 45 (2003).
  - [2] J. A. Shapiro, *Annu. Rev. Microbiol.*, **52**, 81 (1998).
  - [3] Y. Sumino, K. H. Nagai, Y. Shitaka, D. Tanaka, K. Yoshikawa, H. Chaté, and K. Oiwa, *Nature*, **483**, 448 (2012).
  - [4] S. Thutupalli, R. Seemann, and S. Herminghaus, *New J. Phys.*, **13**, 073021 (2011).
  - [5] C. Bechinger, R. D. Leonardo, H. Löwen, C. Reichhardt, G. Volpe, and G. Volpe, *Rev. Mod. Phys.*, **88**, 045006 (2016).
  - [6] M. C. Marchetti, J. F. Joanny, S. Ramaswamy, T. B. Liverpool, J. Prost, M. Rao, R. A. Simha, *Rev. Modern Phys.*, **85**, 1143 (2013).
  - [7] Y. S. Ikura, E. Heisler, A. Awazu, H. Nishimori, and S. Nakata, *Phys. Rev. E*, **88**, 012911 (2013).
  - [8] S. Nakata, M. Nagayama, H. Kitahata, N. J. Suematsu, and T. Hasegawa, *Phys. Chem. Chem. Phys.*, **17**, 10326, (2015).
  - [9] S. Soh, M. Branicki, and B. A. Grzybowski, *Swarming in shallow waters*, *J. Phys. Chem. Lett.* **2**, 770 (2011).
  - [10] S. Tanaka, Y. Sogabe, and S. Nakata, *Phys. Rev. E*, **91**, 032406 (2015).
  - [11] D. Tanaka, *Phys. Rev. Lett.*, **99**, 134103 (2007).
  - [12] N. Shimoyama, K. Sugawara, T. Mizuguchi, Y. Hayakawa, and M. Sano, *Phys. Rev. Lett.*, **76**, 3870 (1996).